



Article

# Delineation of Soil Management Zone Maps at the Regional Scale Using Machine Learning

**Sedigheh Maleki** <sup>1,\*</sup>, **Alireza Karimi** <sup>1</sup> , **Amin Mousavi** <sup>1</sup>, **Ruth Kerry** <sup>2</sup> and **Ruhollah Taghizadeh-Mehrjardi** <sup>3</sup>

<sup>1</sup> Department of Soil Science, Faculty of Agriculture, Ferdowsi University of Mashhad, Mashhad 9177948978, Iran

<sup>2</sup> Department of Geography, Brigham Young University, Provo, UT 84602, USA

<sup>3</sup> Department of Geosciences, University of Tübingen, 72076 Tübingen, Germany

\* Correspondence: smaleki@ferdowsi.um.ac.ir

**Abstract:** Applying fertilizers to soil in a site-specific way that maximizes yields and minimizes environmental damage is an important goal. Developing soil management zones (MZs) is a suitable method for achieving sustainable agricultural production. Thus, this work aims to investigate MZs delineated based on the different soil properties using machine learning methods. To achieve these, 202 soil samples were collected at the agricultural land of pomegranate, pistachio, and saffron. A “random forest” model was applied to map soil properties based on environmental covariates. The predicted “Lin’s concordance correlation coefficient” values in validation soil properties varied from 0.65 to 0.79. The maps indicated low amounts of soil organic carbon, available potassium, available phosphate, and total nitrogen in most of the region. Furthermore, the study identified four different MZs according to relationships between soil properties and environmental covariates. Generally, the ranking of zones in terms of soil fertility was MZ4 > MZ1 > MZ3 > MZ2 based on the investigated soil properties and the soil quality (SQ) map. The five grades of SQ (i.e., very high, high, moderate, low, and very low) indicated that there was heterogeneous SQ in each MZ in the study area. There were 1.65 ha identified in MZ4 with very low SQ. This result is important in determining the amount of fertilizer to add to the soil in the different areas. It confirms the need for more specific regional management of agriculture lands in this region.



**Citation:** Maleki, S.; Karimi, A.; Mousavi, A.; Kerry, R.; Taghizadeh-Mehrjardi, R. Delineation of Soil Management Zone Maps at the Regional Scale Using Machine Learning. *Agronomy* **2023**, *13*, 445. <https://doi.org/10.3390/agronomy13020445>

Academic Editor: Roberto Marani

Received: 17 December 2022

Revised: 30 January 2023

Accepted: 31 January 2023

Published: 2 February 2023



**Copyright:** © 2023 by the authors. Licensee MDPI, Basel, Switzerland. This article is an open access article distributed under the terms and conditions of the Creative Commons Attribution (CC BY) license (<https://creativecommons.org/licenses/by/4.0/>).

## 1. Introduction

Obtaining dense spatial information about soil properties and soil fertility is essential for evaluating the effects of fertilization and irrigation practices on crop production [1]. Moreover, such information is important for determining fertilizer requirements for sustainable soil and crop management [2]. The typical method to manage differences in the soil property variability for agricultural lands is to determine management zones (MZs). MZs are areas with similar soil properties that can be managed uniformly for growing particular crops [3]. Accordingly, defining and optimizing homogeneous MZs is vital to achieve appropriate use of soil and land resources [4]. To improve the efficiency of agricultural management operations, precision agriculture (PA) has developed with the aim of providing a cost-effective way to improve product management and crop productivity and decrease disadvantageous environmental effects of over-application of agrochemicals [5]. PA characterizes soil spatial variability, thereby determining locations where input and various management practices are needed and locations where they are not needed [6]. PA practices normally begin by characterizing soil spatial variation at the field or farm scale. The fields are then divided into MZs. Several types of data and numerical approaches have been used for delineating MZs in PA. Usually inexpensive sensed data related to soil forming properties are used to define MZs such as digital elevation models [7–10], remotely

sensed (RS) imagery [6,11], and electrical conductivity data [12–14]. Khosla et al. [15] suggested that MZs at the scale needed for PA are best determined from multiple sources of sensed data instead of a single source because the environmental covariates that are important to management change from place to place and field to field. Several numerical methods have also been used to determine MZs for PA, such as fuzzy k-means cluster analysis [16,17], principal component analysis (PCA) [18], and soil fertility analysis [19]; however, Vitharana et al. [7] noted that PCA followed by k-means classification has become an almost standard numerical method for determining MZs in PA.

Following on from Khosla et al.'s [15] advice about using several sources of data to determine MZs and corroborating the findings of Vitharana et al. [7], many researchers have used various layers of data to prepare MZs [1,4,9,10,17–21]. However, the data and the numerical techniques used depend on the aims of determining MZs and the scale of the study. In other words, certain data and numerical techniques are more appropriate for digital soil mapping (DSM) to create zones through the field and farm scale, while other data and numerical techniques become more appropriate and important at the regional scale. The data and numerical techniques that are appropriate for defining MZs may also vary with the properties that are being managed. "Clustering algorithms" (CA) were used by Li et al. [22] and Taylor et al. [23] to define MZs. Zeraatpisheh et al. [9] distinguished MZs using "PCA" and "fuzzy c-means" clustering method based on soil biology and topographic indices alongside the soil properties. In this way, Davatgar et al. [19] used PCA and fuzzy CA for appropriating MZs. Zeraatpisheh et al. [10] used soil fertility and soil quality (SQ) grades maps to delineate MZs for the agroecosystem management in southern Iran. Xin-Zhong et al. [24] divided a tobacco farmland in three MZs using geostatistical techniques and some soil fertility variables.

Spatial variability maps of different properties have also been used to delineate homogenous MZs. Representing spatial variability requires extraction of very detailed data concerning agricultural situations, and extracting such data can be very expensive [13]. In order to reduce the impact of traditional management and solve the cost issues linked with adopting more site-specific practices, Tripathi et al. [25] and Moharana et al. [26] have suggested using specific areas of control. These traditional agricultural practices, which presuppose land homogeneity, often result in excess or insufficient fertilizer applications which can reduce productivity and input efficiency [27]. Kerry et al. [8] investigated whether the zones determined using survey, terrain, and yield data were optimal for the simultaneous management of multiple nutrients or soil properties. They noted that often multiple nutrients cannot be effectively managed using the same zones, however, properties that are strongly correlated to more permanent soil properties such as soil texture are more likely to be manageable with one set of MZs.

Information on soil properties, spatial diversity, and soil MZs is still very limited in eastern Iran, especially in the Khorasan Razavi region, which results in uniform management for soil nutrition by farmers in the region. This research aims to (i) accurately map soil properties at the regional scale using statistical analysis and a DSM framework for Bajestan area in eastern Iran, (ii) determine MZs throughout the study area using soil nutrient status, PCA and fuzzy k-means, and (iii) compare the SQ in each MZ to determine if SQ is consistent between MZs. Overall, the findings of this research should result in more efficient fertilizer recommendations and a reduction in production costs due to recommendations being based on MZs and cultivation type.

## 2. Materials and Methods

### 2.1. Study Area

The selected area for study was in Bajestan, a county in Khorasan Razavi province which is located in northeastern Iran. Bajestan has an area of roughly 172,419 ha defined by a rectangle with the following corner coordinates: 34°17'91" to 34°33'79" N and 57°57'56" to 58°00'40" E (Figure 1) and an elevation range of 786–2283 meters above sea level (m a.s.l) [28]. Pomegranate (*Punica granatum* L.), pistachio (*Pistacia vera* L.), and saffron

(*Crocus sativus* L.) are grown in the study area and a variety of landforms and geology are in different parts of the region [28]. According to soil taxonomy [29], the soils are mostly from the Typic Haplocalcids, Typic Torrifluvents, Typic Haplocalcids, and Typic Torripsammets [30].

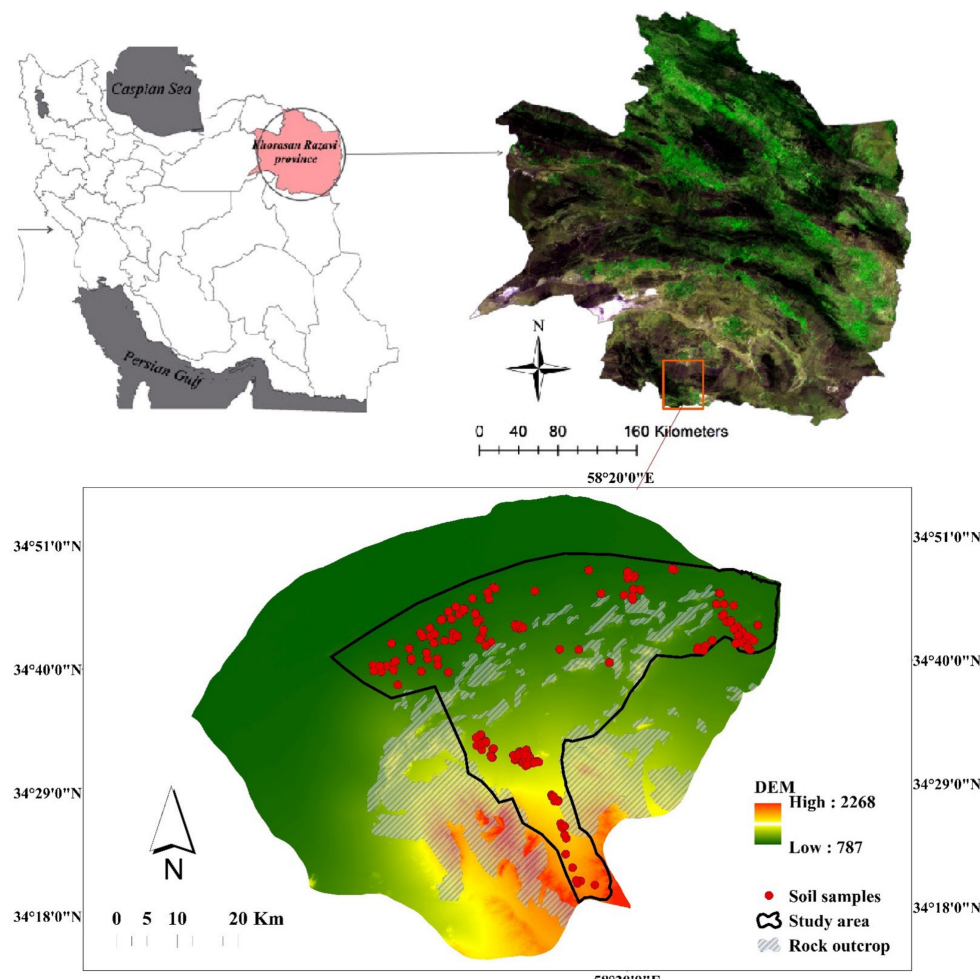


**Figure 1.** Map of the study region in Iran and the soil points within the study region in relation to a digital elevation model (units are meters above sea level).

## 2.2. Procedures

This study completed a series of tasks (Figure 2) including data collection, data analysis and soil property modeling, determination of MZs, statistical analysis, and soil fertility recommendations.

## 2.3. Soil Field and Laboratory Analysis

The soil samples were taken from a depth of 0–30 cm at 202 locations. All soil samples were air-dried and then sieved. The content of calcium carbonate equivalent (CCE) and soil organic carbon (SOC) were evaluated by titration method [31,32]. Standard laboratory measurement methods were used to measure soil acidity (pH) [33], electrical conductivity (EC) [34], soil texture fractions [35], total nitrogen (TN) [36], available phosphate ( $P_{av}$ ) [37], available potassium ( $K_{av}$ ) [38], soluble calcium ( $Ca^{++}$ ), magnesium ( $Mg^{++}$ ), and sodium ( $Na^{+}$ ) [39]. The equation in [40] was used to calculate the amount of sodium adsorption ratio (SAR).

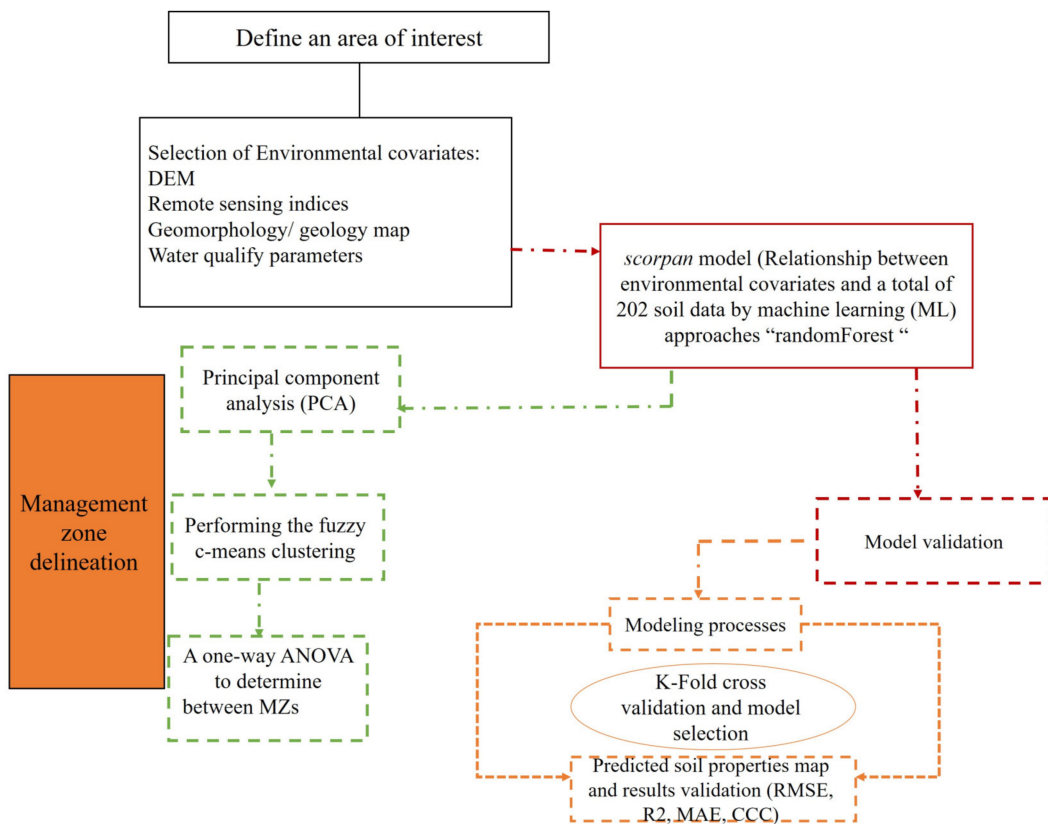


**Figure 2.** Flowchart of stepwise procedure.

#### 2.4. Spatial Variability of Soil Properties

In the current research, the DSM approach [41–45] was used to predict soil properties by analyzing the relationships between environmental covariates and soil properties [45–49]. The environmental covariates used to infer different soil property distributions were tabulated in Table S1. Twenty-one terrain attributes were extracted from a shuttle radar topography mission (SRTM) 1 arc-second DEM (<http://earthexplorer.usgs.gov>, accessed on 15 July 2020) with spatial resolution 30 m. SAGA-GIS version 2.2 was utilized to calculate terrain derivative attributes [50]. RS indices were extracted from Sentinel 2 (<https://sentinel.esa.int/web/sentinel/missions>, accessed on 15 July 2020) imagery [51]. In order to prepare a map of water quality parameters, a total of 190 groundwater features, including qanat and wells, were sampled and analyzed according to standard procedures [52]. Then, spatial analyst of ArcMap GIS was used to generate different useful maps for better understanding the variability of water quality in the study area. Groundwater quality parameters ( $\text{HCO}_3^-$ ,  $\text{Cl}^-$ ,  $\text{SO}_4^{2-}$ ,  $\text{Na}^+$ ,  $\text{Ca}^{++}$ ,  $\text{Mg}^{++}$ , EC, pH, SAR, and TDS) were mapped using geostatistical analysis using the inverse distance weighting (IDW) method [28].

#### 2.5. Random Forests (RF)

Random forests (RF) are decision-tree based models [41,53] which consist of growing sets of trees in the decision tree model [53]. The “ntree” and “mtry” are important parameters that are determined according to number of trees and effective environmental covariates, respectively, in each random subset. The number of environmental covariates can range from one to the total number of independent variables. The number of trees is selected by the user and usually varies from 500 to 1000 [41,53]. It is possible to select the most important effective factors by determining variable importance. The environmental factors with relative importance scores of less than 15% are considered unimportant and are removed from the model [54]. Basically, RF models compute the most important environmental factors by the mean decrease in impurity. The caret package of R3.3.1 was used to predict soil properties for mapping with the RF function [55].

To assess the RF model, a k-fold cross-validation approach was employed. The data were divided into k folds, with one fold serving as the validation set and the remaining k-1 folds used for training. This process was repeated K times, and the average performance was utilized as a metric to evaluate the model. Furthermore, four common indices, including the coefficient of determination ( $R^2$ ), Lin's concordance correlation coefficient (CCC), mean absolute error (MAE), and root mean square error (RMSE), were used to validate the performance of the RF model. Higher  $R^2$  and CCC values and lower MAE and RMSE values show a better model performance based on these validation criteria [56,57].

### 2.6. Delineation of Management Zones (MZs)

To develop MZ classes, principal component analysis (PCA) was first applied to group the variables into principal components in IBM SPSS 22 statistics software. PCs with eigenvalues  $\geq 1.0$  were selected throughout the study area. PCs calculate the maximum variance in a data set by linearly combining the variables and describing the vectors. The fuzzy k-means algorithm was then employed to delineate the study area into different exclusive management areas with the aim of producing homogeneous MZs and statistically minimizing intra-group variability and at the same time maximizing inter-group variability [58]. The MZ analyst software (version 1.0, University of Missouri, Columbia, MO, USA) and the fuzzy k-means clustering FuzME software [59] were used as an unsupervised continuous classification procedure to generate homogeneous MZs [16,60] for dividing farmland into 2 to 7 clusters. This clustering algorithm uses PCs obtained from PCA as input for the cluster analysis. This algorithm creates a continuous grouping of objects with the aim of grouping soil and environmental covariates and assigning partial class membership. A random set of cluster averages results in the membership of each cluster as an iterative process. According to the observation distance to the cluster average, the new averages were re-calculated for each cluster. The settings used in the FuzME software for the study area were as follows: maximum number of repetitions = 300, stop criterion = 0.0001, minimum number of zones = 2, maximum number of zones = 7 and the fuzziness exponent = 1.5 [16,60], respectively. The fuzzy performance index (FPI) and the normalized classification entropy (NCE) were calculated to show the degree of fuzziness and the amount of disorganization to determine the best number of clusters [61]. FPI is the degree of fuzziness created by a specified number of classes and its values may range from 0 to 1. Generally, values close to zero indicate distinct classes with little membership sharing and values close to one indicate distinct classes with a high degree of membership sharing. In addition, the NCE is estimated as the amount of disturbance caused by a certain number of classes. Overall, the lowest membership share (FPI) and the highest amount of organization (NCE) create the best number of clusters [16].

Using IBM SPSS 22 statistics software, descriptive statistics of the studied properties and a one-way analysis of variance were performed using the least significant difference (LSD) test to determine significant heterogeneous changes ( $p \leq 0.05$ ) between MZs [62]. Spatial analysis and mapping of the studied properties was performed in Arc GIS 10.3 software.

## 3. Results and Discussion

### 3.1. Descriptive Statistics for Soil Properties

The mean of EC was  $>4 \text{ dS m}^{-1}$ , indicating that salinity is a major challenge in the area. EC ranged from 0.14 to  $46.46 \text{ dS m}^{-1}$ . In fact, EC values ranged from non-saline to extremely saline (Table 1). This supports past results that indicate there is excessive soil salinity in central Iran [63,64]. The high standard deviation (SD) ( $6.30 \text{ dS m}^{-1}$ ) and coefficient of variation (CV) of 84% emphasize the vast variability of EC in the current study. CVs were categorized as low (<15%), medium (15–35%), high (35–75%), and extremely high (75–150%) variation [65]. The lowest and highest CVs related to pH and  $P_{av}$ , respectively, while the other properties were either high or very high, and sand had moderate CVs (Table 1).

**Table 1.** Descriptive statistical parameters of soil properties of the study area ( $n = 202$ ).

Soil Properties	Min	Max	Mean	SD	Skew.	Kurt.	CV (%)
EC (dS m <sup>-1</sup> )	0.14	46.60	7.50	6.30	2.19	8.57	84.00
pH	6.10	9.10	7.83	0.45	-0.52	2.00	5.75
Sand (%)	22.00	99.50	59.82	14.96	-0.33	-0.42	25.01
Clay (%)	0.00	52.00	13.75	8.58	0.93	2.08	62.40
Silt (%)	0.00	61.20	26.37	14.15	0.13	-0.66	53.66
CCE (%)	2.00	45.00	17.63	7.39	0.92	2.88	41.92
SOC (%)	0.02	2.47	0.56	0.55	1.47	1.51	98.21
TN (g kg <sup>-1</sup> )	0.00	0.24	0.05	0.04	1.36	1.36	80.00
P <sub>av</sub> (mg kg <sup>-1</sup> )	0.20	80.00	10.99	11.83	2.75	10.06	107.64
K <sub>av</sub> (mg kg <sup>-1</sup> )	17.00	695.00	215.51	109.67	1.18	1.95	50.89
Ca <sup>++</sup> (meq L <sup>-1</sup> )	1.50	73.60	22.19	13.61	0.81	1.07	61.33
Mg <sup>++</sup> (meq L <sup>-1</sup> )	0.60	56.00	10.54	7.95	2.59	9.84	75.43
Na <sup>+</sup> (meq L <sup>-1</sup> )	0.46	272.00	43.76	44.37	1.57	3.50	101.39
SAR	0.46	41.00	11.57	9.63	0.76	-0.14	83.23

Min: Minimum; Max: Maximum; SD: Standard deviation; Skew: Skewness; Kurt: Kurtosis; CV: Coefficient of variation; EC: Electrical conductivity; CCE: Calcium carbonate equivalent; SOC: Soil organic carbon; TN: Total nitrogen; P<sub>av</sub>: Available phosphorus; K<sub>av</sub>: Available potassium; Ca<sup>++</sup>: Soluble Ca; Mg<sup>++</sup>: Soluble Mg; Na<sup>+</sup>: Soluble Na; SAR: Sodium adsorption ratio.

Sand, Silt, and CCE showed moderate variability ( $12 \leq CV < 60\%$ ) (Table 1). The high CVs ( $CV \geq 60\%$ ), for EC, clay, SOC, TN, P<sub>av</sub>, Ca<sup>++</sup>, Mg<sup>++</sup>, Na<sup>+</sup> and SAR indicate high variability of nutrients. Additionally, the results of several studies and according to our findings, soil phosphorus had the highest variability [9,24,66] which can be caused by using different phosphorus fertilizers and different management approaches by farmers in areas with diverse cultivation patterns. There was positive skewness ( $>2$ ) and kurtosis ( $>3$ ) for EC values which indicates a non-normal distribution of salinity. The SAR ranged from 0.46 to 41 with a mean of 11.57 which shows that the soils range from extremely sodic to non-sodic levels and had high SD and CV values.

The most significant positive correlations were observed between six variables: TN and SOC ( $r = 0.89$ ), SAR and Na<sup>+</sup> ( $r = 0.85$ ), Na<sup>+</sup> and EC ( $r = 0.78$ ), SAR and EC ( $r = 0.66$ ), Mg<sup>++</sup> and Ca<sup>++</sup> ( $r = 0.60$ ), and P<sub>av</sub> and SOC ( $r = 0.56$ ). Na<sup>+</sup> and EC ( $r = 0.78$ ), SAR and EC ( $r = 0.66$ ), and SAR and Na<sup>+</sup> ( $r = 0.85$ ) illustrated positive correlations (Figure 3). The highest significant negative correlation was observed between silt and sand ( $r = -0.82$ ) (Figure 3) but this is not a true correlation as silt and sand are part of a composition. Other negative correlations were all weak.

### 3.2. Random Forest Prediction Accuracy

The validation results of soil property maps showed the highest  $R^2 = 0.69$  for TN (Table 2). In addition, the validation of map predictions of different soil properties indicated  $R^2 > 0.50$  and CCCs = 0.65–0.79 in the study area. Taghizadeh-Mehrjardi et al. [63], Mulder et al. [67], Gomes et al. [68] and Reddy et al. [57] all reported that an  $R^2 \leq 0.5$  is more common and  $>0.7$  is less common in prediction of soil properties. Therefore, the RF model mapped soil spatial variability well in this study. Additionally, RMSE and MAE results for all soil properties except for K<sub>av</sub> (RMSE = 67.58 and MAE = 46.0) and Na<sup>+</sup> (RMSE = 28.57 and MAE = 18.71) were excellent. There was a very small positive bias for predicted values for all parameters (Table 2) which RMSE and MAE exhibited a positive value with regard to the overestimated prediction of the DSM of soil property. This bias seemed closely related to the average distance of soil sampling, differences of type of cultivated lands and laboratory methods.

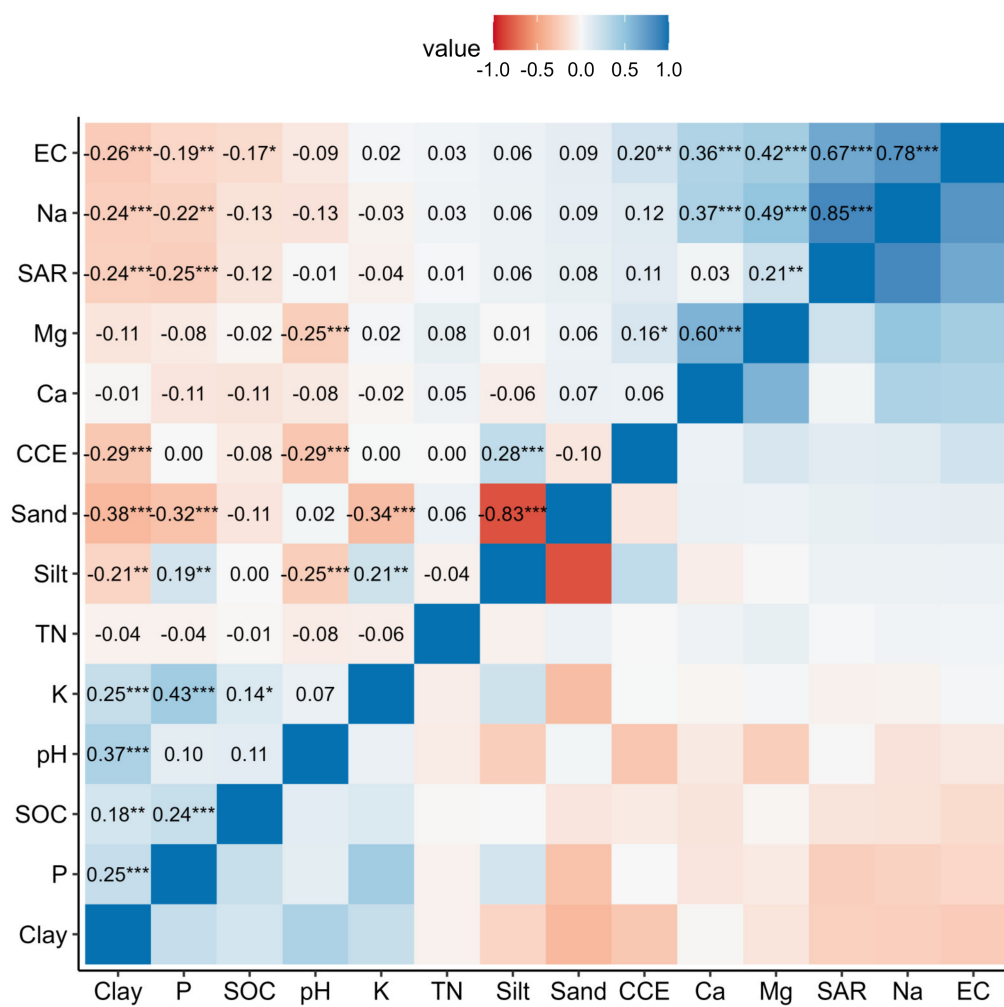


**Figure 3.** Pearson correlation coefficients among soil properties. \*, \*\*, \*\*\* Correlations with  $p > 0.01$  are considered insignificant.

**Table 2.** Validation criteria for soil property predictions using RF models.

Soil Properties	RMSE	MAE	CCC	R <sup>2</sup>
EC (dS m <sup>-1</sup> )	0.08	0.06	0.74	0.62
pH	0.30	0.19	0.67	0.56
Sand (%)	9.00	6.32	0.75	0.64
Clay (%)	5.40	3.52	0.72	0.61
Silt (%)	8.60	6.17	0.75	0.63
CCE (%)	4.41	2.51	0.76	0.65
SOC (%)	0.31	0.21	0.78	0.67
TN (g kg <sup>-1</sup> )	0.02	0.01	0.79	0.69
P <sub>av</sub> (mg kg <sup>-1</sup> )	6.66	4.02	0.78	0.66
K <sub>av</sub> (mg kg <sup>-1</sup> )	67.58	46.00	0.73	0.61
Ca <sup>++</sup> (meq L <sup>-1</sup> )	9.01	6.21	0.66	0.57
Mg <sup>++</sup> (meq L <sup>-1</sup> )	5.35	3.47	0.65	0.56
Na <sup>+</sup> (meq L <sup>-1</sup> )	28.57	18.71	0.71	0.59
SAR	6.31	4.33	0.70	0.57

RMSE: Root mean squared error; MAE: Mean absolute error; R<sup>2</sup>: Coefficient of determination; CCC: Lin's concordance correlation coefficient; EC: Electrical conductivity; CCE: Calcium carbonate equivalent; SOC: Soil organic carbon; TN: Total nitrogen; P<sub>av</sub>: Available phosphorus; K<sub>av</sub>: Available potassium; Ca<sup>++</sup>: Soluble Ca; Mg<sup>++</sup>: Soluble Mg; Na<sup>+</sup>: Soluble Na; SAR: Sodium adsorption ratio.

The high ranges of  $\text{Na}^+$  (Min = 0.46 meq L<sup>-1</sup>, Max = 272.0 meq L<sup>-1</sup>) and  $\text{K}_{\text{av}}$  (Min = 17.0 mg kg<sup>-1</sup>, Max = 695.0 mg kg<sup>-1</sup>) may be the result of different management by farmers in using chemical fertilizer and irrigation water of different qualities. High variations in the distribution of soil particle size influence the capability to retain soluble salts in the soil, and these variations are connected to geological conditions [28]. It may also be that, due to the extent of the study region and limited soil data, using more soil samples in the validation data would improve the  $R^2$ . These results are consistent with other studies that showed good performance by RFs for predicting soil properties with reasonable RMSE and bias [64,69–71]. In this study, the sampling distance was large; therefore, as Jiang et al. [60], de Oliveira et al. [72] and Zeraatpisheh et al. [10] reported, denser sampling may be needed in future studies for more effective soil property mapping.

### 3.3. Spatial Prediction of Soil Properties

The prediction maps of the studied soil properties showed that the north-western part of the study area had the lowest soil pH value (Figure 4a). Low amounts of EC were found in the soils through the center and south of the study area (Figure 4b). The predicted SOC map (Figure 4c) showed that the highest amount is present in the southern parts and in most of the region, especially in the central, north-eastern, and north-western parts of the area, minimal levels of organic carbon were observed. The reason for naturally low amounts of SOC is the arid climate of this region. However, management of the soils by farmers with the use of animal manure or organic fertilizers have caused changes in the amount of SOC in some areas of the study region ( $CV = 98.21\%$ ). The highest and lowest amounts of CCE were found in the north and north-western part and western parts, respectively, which is related to the geology of area (Figure 4d).

Differences in the soil particle size distribution are varied in the region (Figure 4) due to the sediments and soils of this region being affected by different stratigraphic deposits and elevations. The spatial pattern of TN, as shown in Figure 4h, showed a similar pattern to SOC, as exhibited in Figure 4c ( $r = 0.89, p < 0.01$ ). The  $\text{P}_{\text{av}}$  and  $\text{K}_{\text{av}}$  exhibited a low value from the northwest to the northeast and a high value to the south, with a nearly homogeneous spatial pattern over the rest of the study region. Based on the maps of TN,  $\text{P}_{\text{av}}$  and  $\text{K}_{\text{av}}$ , higher values of these three properties were observed in the southern regions (Figure 4i,j). These areas have better conditions for the growth and cultivation of more products such as pomegranate and the highest amount of SOC, which provides the ability to grow a greater variety of crops. Zeraatpisheh et al. [9] expressed the advantages of the prediction map of properties related to soil fertility, including TN,  $\text{P}_{\text{av}}$  and  $\text{K}_{\text{av}}$  to make fertilizer recommendations and showed that areas with the highest amounts of these three properties have better conditions for growing and producing more citrus fruits in the north of Iran and Mazandaran province.

The maps shown in Figure 4, illustrate that the distribution of  $\text{Ca}^{++}$  was very similar to the  $\text{Mg}^{++}$  distribution except in the southern regions, which had higher values of  $\text{Ca}^{++}$ . It seems that low levels of  $\text{Ca}^{++}$  and  $\text{Mg}^{++}$  in the central part of the region frequently occurred where there were low amounts of clay. In addition, due to the relationship between  $\text{Na}^+$  and SAR ( $r = 0.85, p < 0.01$ ), as well as the initial composition of salt, groundwater with alkaline conditions, and the use of alkaline fertilizers in the region, the spatial change maps of  $\text{Na}^+$  and SAR represented a similar distribution in the southern part of the region (Figure 4m,n).

The SAR and EC were high and very high in the northern portion of the region where pistachio is grown (Figure 4). Groundwater quality maps (based on SAR,  $\text{Na}^+$ , TDS,  $\text{Cl}^-$ , EC,  $\text{Ca}^{++}$ , and  $\text{Mg}^{++}$ ) reveal that the associated groundwater parameters are also high in the same area [28]. Cultivated lands of the north are in close proximity of Bajestan playa (Kavir-e Namak), which is another important factor that contributes to high salinity and SAR in this area. This is particularly true in the northwestern part of the region. This is the location of the saltiest part of the playa. Maleki et al. [28] and Taghizadeh-Mehrjardi et al. [63] reported similar findings in studies of the variation of soil properties in the

Bajestan region and soil salinity prediction in the Ardakan region of Yazd Province. In some sections of the northern part of the region, heavy soil texture (clay) also increases salt retention. Improper water management on irrigated cultivated lands in northern Bajestan that have low slopes and poor natural drainage has enhanced the salinity of groundwater, changed the depth of the water table, and salinized the soils above it. Raiesi [73] and Nabiollahi et al. [71] highlighted the role of increasing soil salinity in decreasing SQ in arid and semiarid regions. Groundwater and gradual salinization of soil have been observed in the study area. Bhutta and Alam [74] showed that saline soils increased by approximately 17 million ha (from 56% to 73%) between 1953–1954 and 2001–2003 due to the dropping water table and increased salinity from over-pumping of groundwater.

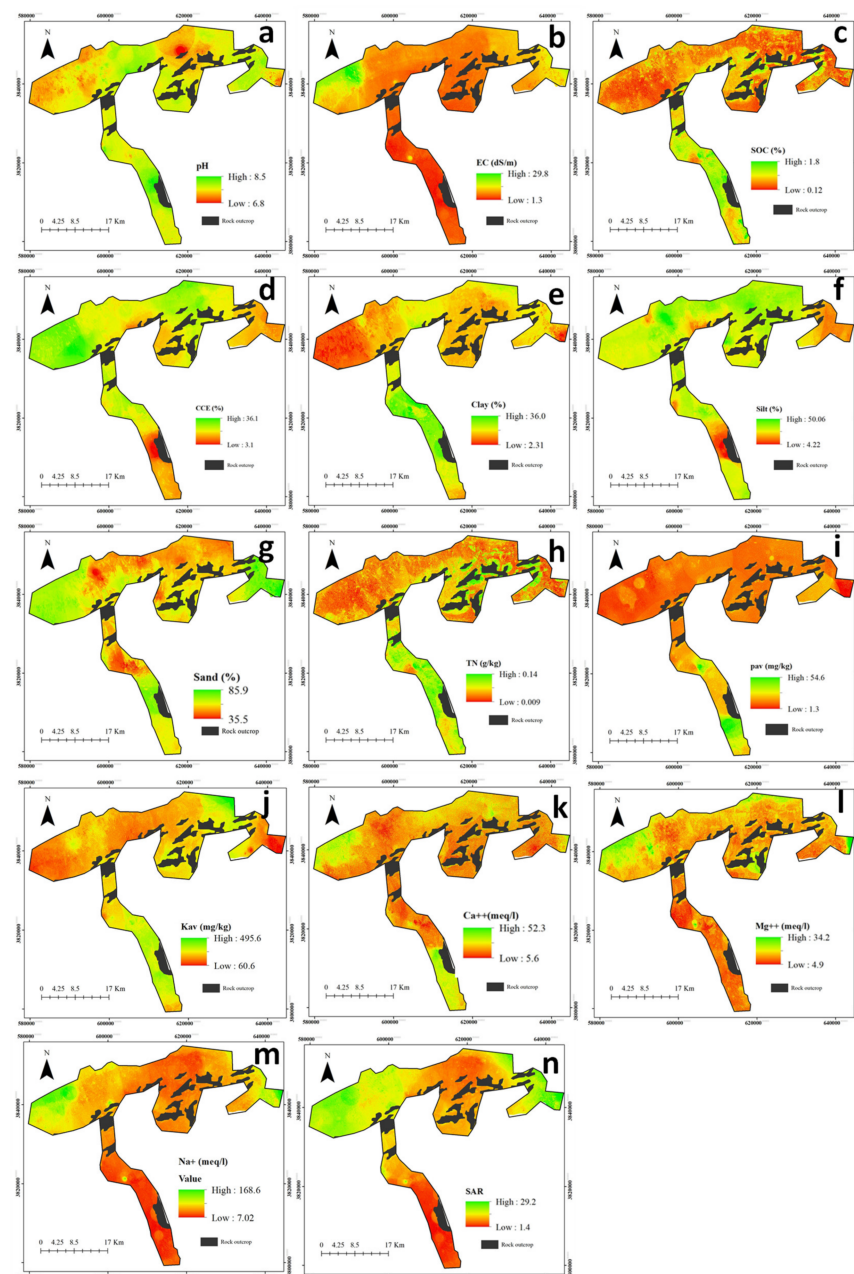


**Figure 4.** Maps showing the spatial distribution for all studied soil properties in 0–30 cm: (a) pH, (b) electrical conductivity ( $\text{EC, dS m}^{-1}$ ); (c) soil organic carbon (SOC, %); (d) calcium carbonate equivalent (CCE, %); (e) clay (%); (f) silt (%); (g) sand (%); (h) total nitrogen (TN, %); (i) available phosphorus ( $\text{P}_{\text{av}}, \text{mg kg}^{-1}$ ); (j) available potassium ( $\text{K}_{\text{av}}, \text{mg kg}^{-1}$ ); (k)  $\text{Ca}^{++}$ : soluble Ca ( $\text{meq L}^{-1}$ ); (l)  $\text{Mg}^{++}$ : soluble Mg; (m)  $\text{Na}^{+}$ : soluble Na; (n) SAR: sodium adsorption ratio.

### 3.4. Principal Component Analysis (PCA)

As shown in Table 3, PCA is a good method for summarizing parameter effects because of the high correlation between some soil properties. PCs with eigenvalues  $>1.0$  represented 73.76% of the dataset variability in the study area (Table 3). PC1 accounted for most of the total data variance (25.68%), with the strongest positive loading factors for EC,  $\text{Na}^+$ , and SAR. The map of PC1 showed the high values in north and northeastern parts of the study area (Figure 5a) similar to SAR,  $\text{Na}^+$ , and EC distribution (Figure 4). PC2 explained 17.27% of the total variance and had the strongest loadings for sand (large negative loading factor) and silt (large positive loading factor). The higher values of PC2 (Figure 5b) coincide with the sand map (Figure 4). PC3 had the strongest loadings for SOC, TN,  $\text{P}_{\text{av}}$ , and  $\text{K}_{\text{av}}$  and had positive loading factors that explained another 12.43% of the total variance of the dataset. PC3 has high values in part of the southern area (Figure 5c) where TN and SOC maps showed the higher values. PC4 explained 9.40% of the data variation with strong positive loading factors for pH and clay and negative loading factors for CCE (Table 3) and the distribution map of PC4 (Figure 5d) showed similar changes to the mentioned soil properties maps (Figure 4). The last PC (PC5) described 8.96% of the data variability with a positive loading factor for  $\text{Ca}^{++}$  and  $\text{Mg}^{++}$  (Table 3 and Figure 5e). Thus, five principal components (PC1, PC2, PC3, PC4, and PC5) were used to delineate the MZs for the study region. Davatgar et al. [19] used PCA and “fuzzy k-means” to distinguish MZs for a paddy field in the north of Iran and reported that 72.95% of soil property changes were described by three PCs. Zeraatpisheh et al. [9], in a study in Iran, used PCA and fuzzy c-means to define soil MZs in citrus orchards and stated that four PCs could explain 78.66% of the variation in soil properties. Accordingly, the PCA method incorporated 14 input variables into five new PCs which explain most of the spatial variation of these properties.

**Table 3.** Results of principal components analysis (PCA) of soil properties ( $n = 202$ ).

	PC1	PC2	PC3	PC4	PC5
Proportion of variance %	25.68	17.27	12.43	9.40	8.96
Cumulative proportion of variance %	25.68	42.95	55.39	64.79	73.76
Eigenvalues	4.10	2.76	1.98	1.50	1.43
EC ( $\text{dS m}^{-1}$ )	<b>0.81</b>	-0.04	-0.16	-0.13	0.25
pH	0.06	-0.14	0.07	<b>0.69</b>	-0.20
Sand (%)	0.05	<b>-0.94</b>	-0.10	0.00	0.03
Clay (%)	-0.16	0.29	0.31	<b>0.69</b>	0.09
Silt (%)	0.04	<b>0.82</b>	-0.08	-0.42	-0.09
CCE (%)	0.12	0.04	-0.01	<b>-0.72</b>	-0.01
SOC (%)	-0.18	0.06	<b>0.87</b>	0.21	-0.02
TN ( $\text{g kg}^{-1}$ )	-0.22	0.05	<b>0.84</b>	0.14	0.03
$\text{P}_{\text{av}}$ ( $\text{mg kg}^{-1}$ )	-0.14	0.18	<b>0.56</b>	-0.04	-0.08
$\text{K}_{\text{av}}$ ( $\text{mg kg}^{-1}$ )	0.09	0.28	<b>0.73</b>	0.04	0.02
$\text{Ca}^{++}$ ( $\text{meq L}^{-1}$ )	0.15	-0.04	-0.07	-0.01	<b>0.94</b>
$\text{Mg}^{++}$ ( $\text{meq L}^{-1}$ )	0.46	-0.00	0.34	-0.25	<b>0.61</b>
$\text{Na}^+$ ( $\text{meq L}^{-1}$ )	<b>0.90</b>	-0.00	-0.14	-0.07	0.24
SAR	<b>0.87</b>	-0.01	-0.23	0.00	-0.11

Values in bold correspond, for each variable, to the factor for which the PC value is the largest. Extraction method: Principal component analysis (PCA); EC: Electrical conductivity; CCE: Calcium carbonate equivalent; SOC: Soil organic carbon; TN: Total nitrogen;  $\text{P}_{\text{av}}$ : Available phosphorus;  $\text{K}_{\text{av}}$ : Available potassium;  $\text{Ca}^{++}$ : Soluble Ca;  $\text{Mg}^{++}$ : Soluble Mg;  $\text{Na}^+$ : Soluble Na; SAR: Sodium adsorption ratio.

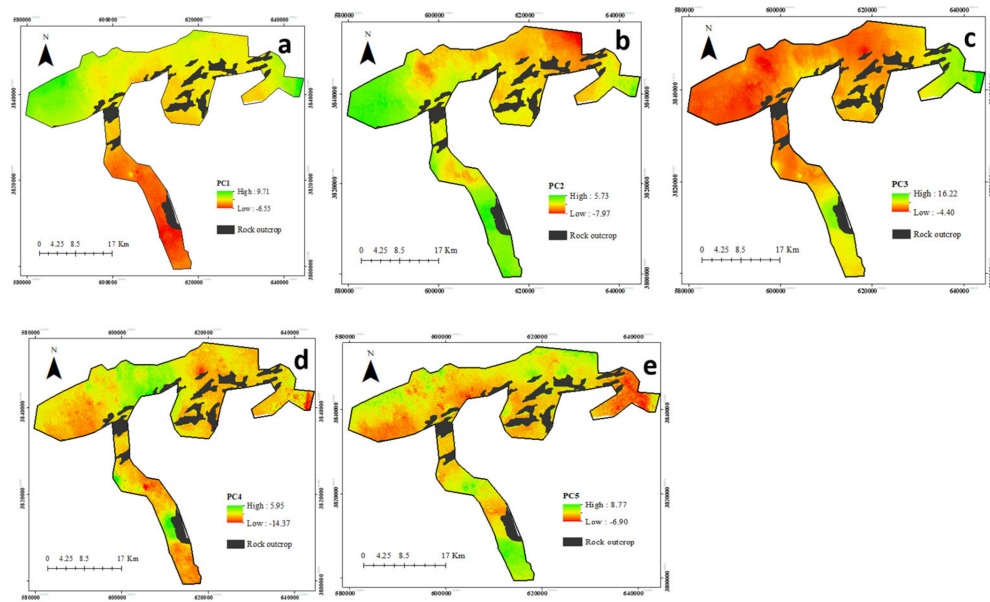


**Figure 5.** Maps showing the spatial distribution of the PCs for all studied soil properties in 0–30 cm: (a) PC1; (b) PC2; (c) PC3; (d) PC4; (e) PC5.

### 3.5. Clustering Analysis

Five PCs were used with cluster analysis to define MZs. The FuzMe software was used to run the “fuzzy k-means” clustering on the five PCs. This method allows differentiation between different areas with similar properties. Hence, when the FPI and NCE values were negligible, the optimal number of MZs could be distinguished, as shown in Figure 6. Four MZs were chosen as optimal as this is where the FPI is at a minimum and NCE is at its second-lowest value. A one-way analysis of variance (ANOVA) was performed to assess the effectiveness of the combination of the PCA clustering algorithm and “fuzzy k-means” to delineate MZs as well as their spatial variability. The four different MZs that were distinguished as the optimal are shown in Figure 7. Several studies reported good results using the analysis of variance to delineate areas [18,61,75]. Zeraatpisheh et al. [9] performed a recent study where two MZs were detected by the fuzzy k-means method in an area in Darab city, Iran.

Based on the results obtained from Table 4, there were significant differences ( $p < 0.05$ ) between some soil properties except for sand, SOC, TN,  $P_{av}$ , and  $Ca^{++}$  for the four MZs. In comparison to other MZs, pH showed a significant difference in MZ4; clay and  $K_{av}$  showed significant differences in MZ3; and  $Mg^{++}$ ,  $Na^+$ , and SAR showed a significant difference in MZ2. MZ3 had lower clay and SOC values and could have lower potential soil fertility than the other zones. This suggests that in this area, more chemical fertilizers and organic fertilizers are needed to increase SOC in MZ3. Generally, the ordering of MZs was MZ4 > MZ1 > MZ3 > MZ2 in relation to soil fertility for all investigated soil properties, based on the results in Table 4. These results can be useful for deciding how to distribute fertilizer in each zone with an emphasis on regionally specific decision making for agriculture lands to allow more sustainable production and, in turn, to reduce environmental risks from uneven application of chemical fertilizers.

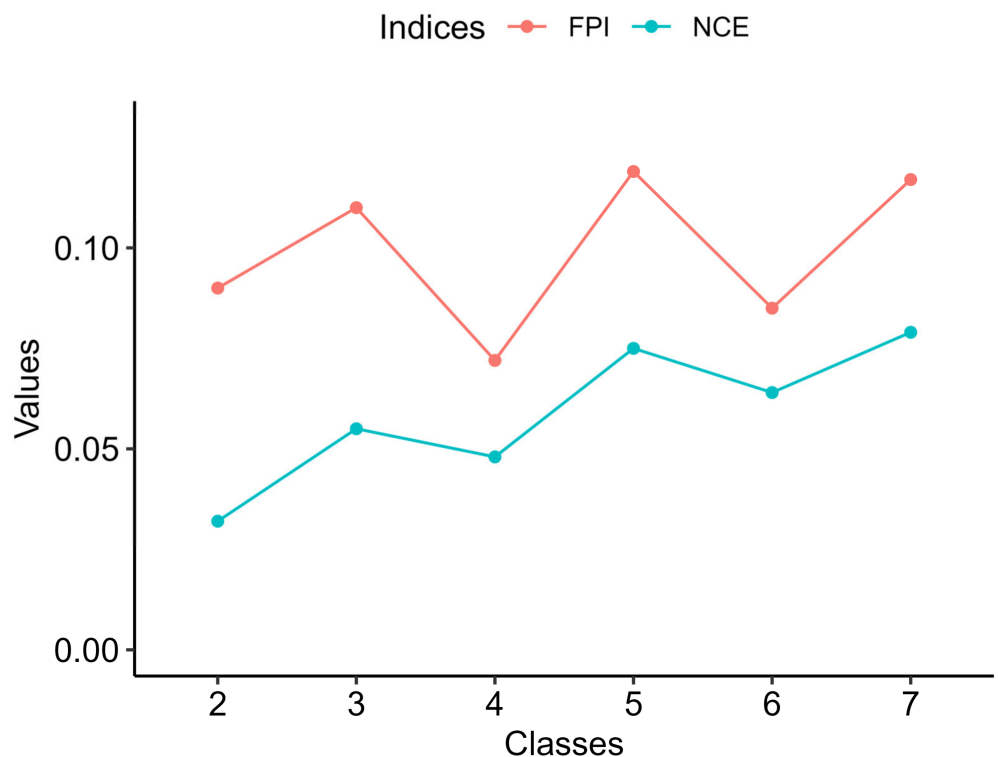


**Figure 6.** Fuzziness performance index (FPI) and normalized classification entropy (NCE) for the different number of cluster classes defined by PCA and fuzzy k-means.

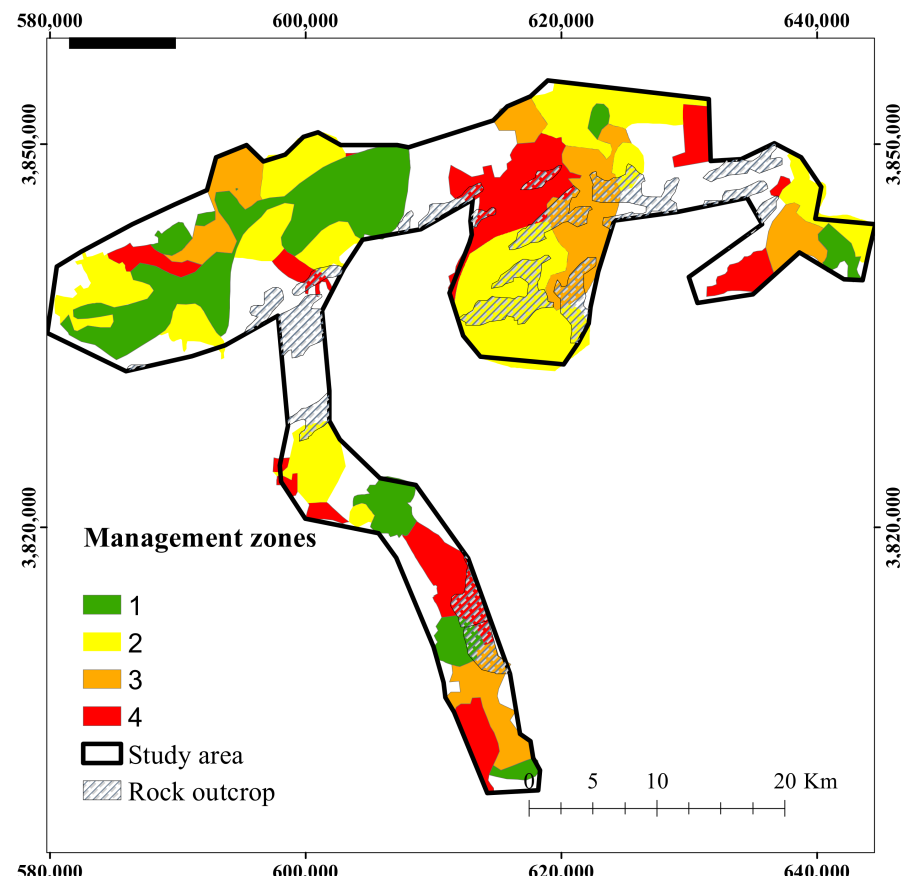


**Figure 7.** The management zones map in the study area. White areas are non-agricultural lands.

**Table 4.** Mean values for each management zone and analysis of variance for all studied soil properties.

Soil Properties	MZ1	MZ2	MZ3	MZ4
n	90	48	22	42
EC ( $\text{dS m}^{-1}$ )	6.51 b	10.45 a	7.78 ab	6.10 b
pH	7.79 b	7.77 b	7.71 b	8.03 a
Sand (%)	59.99 a	60.15 a	57.55 a	60.24 a
Clay (%)	13.34 ab	14.03 ab	10.47 b	16.01 a
Silt (%)	26.60 ab	25.76 ab	31.94 a	23.64 b
CCE (%)	18.36 b	17.07 bc	21.73 a	14.56 c
SOC (%)	0.64 a	0.43 a	0.38 a	0.62 a
TN ( $\text{g kg}^{-1}$ )	0.05 a	0.03 a	0.04 a	0.05 a
P <sub>av</sub> ( $\text{mg kg}^{-1}$ )	11.53 a	9.26 a	12.23 a	11.14 a
K <sub>av</sub> ( $\text{mg kg}^{-1}$ )	194.86 b	219.91 b	291.90 a	214.73 b
Ca <sup>++</sup> ( $\text{meq L}^{-1}$ )	20.58 a	25.73 a	21.85 a	21.77 a
Mg <sup>++</sup> ( $\text{meq L}^{-1}$ )	9.49 b	14.51 a	10.05 b	8.51 b
Na <sup>+</sup> ( $\text{meq L}^{-1}$ )	35.98 b	70.43 a	46.30 b	28.60 b
SAR	9.96 b	16.15 a	11.81 b	9.64 b

Means with the same letter are not significantly different at the 0.05 probability level based on the least significant difference test. EC: Electrical conductivity; CCE: Calcium carbonate equivalent; SOC: Soil organic carbon; TN: Total nitrogen; P<sub>av</sub>: Available phosphorus; K<sub>av</sub>: Available potassium; Ca<sup>++</sup>: Soluble Ca; Mg<sup>++</sup>: Soluble Mg; Na<sup>+</sup>: Soluble Na; SAR: Sodium adsorption ratio.

### 3.6. Management Zones (MZs) and Fertilizer Recommendation

Figure 7 shows the MZ map with four MZs. ANOVA was used to evaluate differences in soil nutrients among MZs. There was a significant difference ( $p < 0.05$ ) between the MZs for each of the soil properties (Table 4). Soils in MZ4 with higher values of clay and SOC and lower values of EC and SAR showed higher soil fertility potential than other zones. There was greater variability in EC and SAR between MZs (Table 4). Mean EC values in MZ2 and MZ3 were 10.45 and 7.78  $\text{dS m}^{-1}$ , respectively. Similar to EC, the highest values of SAR were found under MZ2 and MZ3 with values greater than 10. The greatest TN, P<sub>av</sub>, and K<sub>av</sub> deficiencies occurred in MZ2. The most common reason for these deficiencies in this unit could be the result of reduced capacity of mineral fertilizers and insufficient clay content in this zone. It appears that native N input (low OC) and higher N reduction by leaching (low clay content) limited MZs.

MZ3 contained P<sub>av</sub> and K<sub>av</sub> around 12.23 and 291.90  $\text{mg kg}^{-1}$  with these areas appearing to have sufficient soil nutrients. MZ4 has the best intrinsic soil fertility due to higher clay, SOC, and nutrient reserves. However, the area of this zone was 16,211.32 ha and MZ2 had the highest area at about 24,580.50 ha (Figure 7).

Maleki et al. [43] predicted SQ maps in earlier study using two datasets (total data set–TDS and minimum data set–MDS) by linear (L) and nonlinear (NL) scoring methods from 223 surface soil samples (0–30 cm depth). The results of the soil quality indices (SQIs) map indicated the maximum values of the SQIs in the southern and central parts of the study area, while the minimum values were found in the north of the study area due to higher EC and SAR. The DSM-predicted soil property maps generated here were transformed to SQI maps according to Maleki et al. [43] and were classified into five classes of SQ including very high (I), high (II), moderate (III), low (IV), and very low (V). The area of MZs within each SQ grade is presented in Table 5. The findings indicate that there are different SQ grades within each of the four delineated zones.

**Table 5.** Area of soil quality (SQ) grade within each management zone.

Quality Index	SQI Range	MZ1	MZ2	MZ3	MZ4
I (very high)	>0.639	0.47 (0.003%)	-	0.08 (0.0006%)	-
II (high)	0.529–0.639	1004 (6.38%)	166 (0.68%)	440 (3.52%)	828 (5.10%)
III (moderate)	0.418–0.529	5903 (37.48%)	16475 (67.02%)	7749 (62.0%)	10518 (64.88%)
IV (low)	0.307–0.418	8780 (55.72%)	7931 (32.27%)	4289 (34.33%)	4863 (30%)
V (very low)	<0.307	66 (0.41%)	7.6 (0.03%)	18 (0.15%)	1.65 (0.0001)

MZ4 had an area of 16211.32 ha, the largest area, categorized as moderate (III) SQ; although part of the area was in the high class (II) SQ (area of 828.21 ha), while the lowest area of very low (V) SQ was located in MZ4 (Table 5). In contrast, MZ1 contained five SQ grades (Table 5) with 0.47 ha located in very high (I) SQ and 66.16 in very low (V).

The results for SQ maps [43] showed that the lower grades of SQ with the highest EC and SAR levels were in the northern portion of the study area in proximity to the playa where elevations are the lowest and topographic wetness index (TWI) is highest [76]. Soil salinity and alkalinity are subject to two primary and secondary factors in the study area. The primary agent includes the conditions of the physical environment (climate, geology, and topography). The secondary factor includes the human uses of the land and management practices (particularly the use of poor-quality irrigation water and inadequate agricultural operation that increase the likelihood of salinity, alkalinity, and sodicity).

The results of Table 6 show the main restricted indicators in each MZ regarding SQI. According to the results of SQ and MZs (Table 6), prescription of fertilizer should be applied based on the uniform fertilization management within each SQ or MZ area. It should be noted that determining the amount of fertilizer required in each region is based on available and common fertilizers used by farmers in the region. Reducing production costs, increasing the quantity and quality of the product, and keeping the environment and soil safe from pollution are potential advantages of fertilizing based on specialized prescriptions and in line with sustainable agricultural practices. Numerous researchers have also reported the distribution of different fertilizers based on MZ delineation [9–11,18,19,72].

**Table 6.** The restricted limitation of management zones (MZs) related to the area of soil quality (SQ) and land improvement by comparing the difference between site-specific fertilization and uniform management.

MZs	Largest Extent of SQI	Restricted Indicators	Suggested Land Improvement
MZ1	II and III > 70%	Lack of soil nutrient especially TN and P <sub>av</sub>	Use of chemical fertilizers (i.e., urea, 46%; triple superphosphate, 46%) and animal manure, leaving plant residuals on the ground
MZ2	III and IV > 99%	Lack of SOC, soil nutrient especially TN, P <sub>av</sub> , K <sub>av</sub> , and high salinity and SAR	Use of chemical fertilizers (i.e., urea, 46%; triple superphosphate, 46%; potassium sulfate, 46%), sulfur (with 50% purity), and animal manure, leaving plant residuals on the ground
MZ3	III and IV > 96%	Lack of SOC, soil nutrient especially TN, P <sub>av</sub> , K <sub>av</sub> , and high salinity and SAR	Use of chemical fertilizers (i.e., urea, 46%; triple superphosphate, 46%; potassium sulfate, 46%), sulfur (with 50% purity), and animal manure, leaving plant residuals on the ground
MZ4	II and III > 75%	Lack of soil nutrient especially TN and P <sub>av</sub>	Use of chemical fertilizers (i.e., urea, 46%; triple superphosphate, 46%) and animal manure, leaving plant residuals on the ground

The fertilization method is very important in the nutritional management of plants. Fertilization should be performed in such a way that the elements required by the plant are provided to the plant in a suitable form and at the desired time. Various factors, such as the type of fertilizer and plant species, affect the fertilization method. In addition, the

amount and time for the applied fertilizers will be different in different regions. To increase the efficiency of fertilizers, the management approach and method of consumption have been taken into consideration. The amount of phosphorus in the region is relatively low to medium; in general, it indicates the relative poverty of this element in the soils of the region. However, the deficiency is not as severe as nitrogen ( $TN < 0.05$ ). Therefore, nitrogen fertilizer consumption should be given serious attention. In order to achieve the highest absorption efficiency of chemical fertilizers for phosphorus, it should be used at the right time and according to the needs of the plant.

The results in Table 4 show that the amount of potassium is relatively moderate amount with a significant difference in terms of this element in MZ3 (Table 6) and other cases (probably due to the difference in soil texture and cultivation pattern). Potassium plays an important role in plant resistance to disease. Among its other important roles, it is possible to regulate the work of stomata openings and water relations and accelerates the growth of generative tissues. Most importantly, the special conditions of the region, which is under the stress of drought, wind, and sometimes cold, should be considered. Therefore, it is necessary to use potassium in the form of potassium sulfate fertilizer in the soils of the region.

The findings showed that farmlands in the study area are generally lacking in SOC ( $<0.70\%$ ), especially in MZ2 and MZ3 with the low amount  $<0.40$  (Tables 4 and 6). The lack of SOC is one of the most notable problems of the study region. Considering the importance of soil organic matter, increasing it as the first priority for improving soil fertility in plant nutrition management should be given serious attention (Table 6).

Annual applications of gypsum or liquid organic sulfur and organic fertilizers in appropriate ratios to promote effective leaching of salt may be a highly effective approach to remediation of saline and sodic soils. Determining the appropriate cultivation pattern based on MZ maps and changing cultivation towards greenhouse crops can lead to sustainable agriculture and prevent soil degradation. Recognition of the importance of irrigation, water quality, and the patterns of SQ predictions on the MZs map provides scientific guidance for enhanced management of the soils of the Bajestan area, for developing more sustainable agricultural practices. This approach can also be applied in similar regions through DSM.

#### 4. Conclusions

It is necessary to check the fertility status of the soil over time to prevent the depletion of elements from the soil and to replace them at appropriate levels. However, monitoring the soil fertility status should be performed using a low-cost technique and input data so that farmers know which areas have similar production potential. The optimal number of MZs was determined to be four by PCA and the “fuzzy k-means” method. A one-way ANOVA demonstrated significant differences between different MZs in terms of the measured soil properties. The soil fertility indices measured in this case study demonstrated that the low amount of SOC, TN,  $P_{av}$ , and  $K_{av}$  appear to be the main restriction of sustainable production, due to the lower TN,  $P_{av}$ , and  $K_{av}$  of the soil. Application of mineral fertilizers N, P, and K is therefore needed. N, P, and K management are crucial to keep the crop yield at a high level. Moreover, these results showed that by reducing the variability within the zone, the development of MZs through cluster analysis will allow farmers to use more site-specific management. Average soil nutrient values can be used as a guide to calculate the ratio of fertilizer distribution in different areas. Nevertheless, incorporating yield values into this system could improve the rate and timing of fertilizer applications. Generally, as an inexpensive approach to predicting soil properties over large areas and subsequently determining MZs is suggested as a way to improve the accuracy of maps and decrease soil sampling.

Every farmer is faced with different cost strategies and different performance levels for fertilizer use. Based on the available capital, the farmer considers a cost of buying different fertilizers in order to reach a certain performance goal, which creates a different amount of nutrients for the soil. The results of this study will help the farmer to choose the optimal

fertilizer combination. Therefore, the optimal amount of fertilizer should be determined considering the soil analysis tests.

**Supplementary Materials:** The following supporting information can be downloaded at: <https://www.mdpi.com/article/10.3390/agronomy13020445/s1>, Table S1: List of environmental covariates for digital soil mapping.; References [77–92] are cited in Supplementary Materials.

**Author Contributions:** Conceptualization, S.M. and A.K.; methodology, S.M.; R.T.-M. and A.K.; software, S.M., A.M. and R.T.-M.; validation, S.M. and R.T.-M.; formal analysis, S.M., A.K. and R.T.-M.; investigation, S.M. and A.K.; resources, S.M. and A.K.; data curation, S.M.; writing—original draft preparation, S.M., A.K., A.M. and R.K.; writing—review and editing, S.M., A.K., A.M., R.T.-M. and R.K.; visualization S.M. and R.T.-M.; supervision, S.M., A.K. and R.T.-M. Project administration, S.M.; funding acquisition, S.M. All authors have read and agreed to the published version of the manuscript.

**Funding:** Sedigheh Maleki was partially supported by a grant from Ferdowsi University of Mashhad, Iran (NO. FUM- 14002794075).

**Data Availability Statement:** The dataset used in this project can be available from the corresponding author on reasonable request.

**Acknowledgments:** The authors are very grateful to Ferdowsi University of Mashhad and Management of Agricultural Jihad in Bejastan for their financial support and help in soil sampling, respectively.

**Conflicts of Interest:** The authors declare no conflict of interest.

## References

- Yao, R.J.; Yang, J.S.; Zhang, T.J.; Gao, P.; Wang, X.P.; Hong, L.Z.; Wang, M.W. Determination of site-specific management zones using soil physico-chemical properties and crop yields in coastal reclaimed farmland. *Geoderma* **2014**, *232*, 381–393. [[CrossRef](#)]
- Peralta, N.R.; Costa, J.L.; Balzarini, M.; Franco, M.C.; Córdoba, M.; Bullock, D. Delineation of management zones to improve nitrogen management of wheat. *Comput. Electron. Agric.* **2015**, *110*, 103–113. [[CrossRef](#)]
- Ferguson, R.B.; Lark, R.M.; Slater, G.P. Approaches to management zone definition for use of nitrification inhibitors. *Soil Sci. Soc. Am. J.* **2003**, *67*, 937–947. [[CrossRef](#)]
- Castrignanò, A.; Buttafuoco, G.; Quarto, R.; Parisi, D.; Rossel, R.V.; Terribile, F.; Langella, G.; Venezia, A. A geostatistical sensor data fusion approach for delineating homogeneous management zones in Precision Agriculture. *Catena* **2018**, *167*, 293–304. [[CrossRef](#)]
- Franzen, D.W.; Hopkins, D.H.; Sweeney, M.D.; Ulmer, M.K.; Halvorson, A.D. Evaluation of soil survey scale for zone development of site specific nitrogen management. *Agron. J.* **2002**, *94*, 381–389.
- Fraisse, C.W.; Sudduth, K.A.; Kitchen, N.R.; Fridgen, J.J. Use of unsupervised clustering algorithms for delineating within-field management zones. In Proceedings of the International Meeting, Toronto, ON, Canada, 18–21 July 1999; American Society of Agricultural Engineers: St. Joseph, MI, USA, 1999.
- Vitharana, U.W.A.; Van Meirvenne, M.; Simpson, D.; Cockx, L.; De Baerdemaeker, J. Key soil and topographic properties to delineate potential management classes for precision agriculture in the European loess area. *Geoderma* **2008**, *143*, 206–215. [[CrossRef](#)]
- Kerry, R.; Ingram, B.; Oliver, M. Sampling needs to establish effective management zones for plant nutrients in precision agriculture. In *Precision Agriculture*, 1st ed.; Wageningen Academic Publishers: Wageningen, The Netherlands, 2021; pp. 177–192.
- Zeraatpisheh, M.; Bakhshandeh, E.; Emadi, M.; Li, T.; Xu, M. Integration of PCA and fuzzy clustering for delineation of soil management zones and cost-efficiency analysis in a citrus plantation. *Sustainability* **2020**, *12*, 5809. [[CrossRef](#)]
- Zeraatpisheh, M.; Bottega, E.L.; Bakhshandeh, E.; Owliaie, H.R.; Taghizadeh-Mehrjardi, R.; Kerry, R.; Scholten, T.; Xu, M. Spatial variability of soil quality within management zones: Homogeneity and purity of delineated zones. *Catena* **2022**, *209*, 105835. [[CrossRef](#)]
- Breunig, F.M.; Galvão, L.S.; Dalagnol, R.; Dauve, C.E.; Parraga, A.; Santi, A.L.; Della Flora, D.P.; Chen, S. Delineation of management zones in agricultural fields using cover-crop biomass estimates from PlanetScope data. *Int. J. Appl. Earth Obs. Geoinf.* **2020**, *85*, 102004. [[CrossRef](#)]
- Cambouris, A.N.; Nolin, M.C.; ZebARTH, B.J.; Laverdiere, M.R. Soil Management Zones Delineated by Electrical Conductivity to Characterize Spatial and Temporal Variations in Potato Yield and in Soil Properties. *Am. J. Potato Res.* **2006**, *83*, 381–395. [[CrossRef](#)]
- Medeiros, W.N.; de Queiroz, D.M.; Valente, D.S.M.; Pinto, F.D.A.; Melo, C.A.D. The temporal stability of the variability in apparent soil electrical conductivity. *Biosci. J.* **2016**, *32*, 150–159. [[CrossRef](#)]

14. De Assis Silva, S.; Oliveira dos Santos, R.; Marçalde Queiroz, D.; Soares de Souza Lima, J.; Fraga Pajehú, L.; Carvalho Medauar, C. Apparent soil electrical conductivity in the delineation of management zones for cocoa cultivation. *Inf. Process. Agric.* **2022**, *9*, 443–455. [[CrossRef](#)]
15. Khosla, R.; Inman, D.; Westfall, D.G.; Reich, R.M.; Frasier, M.; Mzuku, M. A synthesis of multi-disciplinary research in precision agriculture: Site-specific management zones in the semi-arid western Great Plains of the USA. *Precis. Agric.* **2008**, *9*, 85–100. [[CrossRef](#)]
16. Fridgen, J.J.; Kitchen, N.R.; Sudduth, K.A.; Drummond, S.T.; Wiebold, W.J.; Fraisse, C.W. Management zone analyst (MZA) software for subfield management zone delineation. *J. Agron.* **2004**, *96*, 100–108.
17. Gili, A.; Álvarez, C.; Bagnato, R.; Noellemyer, E. Comparison of three methods for delineating management zones for site-specific crop management. *Comput. Electron. Agric.* **2017**, *139*, 213–223. [[CrossRef](#)]
18. Schenatto, K.; De Souza, E.G.; Bazzi, C.L.; Gavioli, A.; Betzek, N.M.; Beneduzzi, H.M. Normalization of data for delineating management zones. *Comput. Electron. Agric.* **2017**, *143*, 238–248. [[CrossRef](#)]
19. Davatgar, N.; Neishabouri, M.R.; Sepaskhah, A.R. Delineation of site specific nutrient management zones for a paddy cultivated area based on soil fertility using fuzzy clustering. *Geoderma* **2012**, *173*, 111–118. [[CrossRef](#)]
20. Gavioli, A.; de Souza, E.G.; Bazzi, C.L.; Schenatto, K.; Betzek, N.M. Identification of management zones in precision agriculture: An evaluation of alternative cluster analysis methods. *Biosyst. Eng.* **2019**, *181*, 86–102. [[CrossRef](#)]
21. Iticha, B.; Takele, C. Digital soil mapping for site-specific management of soils. *Geoderma* **2019**, *351*, 85–91. [[CrossRef](#)]
22. Li, Y.; Shi, Z.; Li, F.; Li, H.Y. Delineation of site-specific management zones using fuzzy clustering analysis in a coastal saline land. *Comput. Electron. Agric.* **2007**, *56*, 174–186. [[CrossRef](#)]
23. Taylor, J.C.; Wood, G.A.; Earl, R.; Godwin, R.J. Soil factors and their influence on within-field crop variability, part II: Spatial analysis and determination of management zones. *Biosyst. Eng.* **2003**, *84*, 441–453. [[CrossRef](#)]
24. Xin-Zhong, W.; Guo-Shun, L.; Hong-Chao, H.; Zhen-Hai, W.; Qing-Hua, L.; Xu-Feng, L.; Wei-Hong, H.; Yan-Tao, L. Determination of management zones for a tobacco field based on soil fertility. *Comput. Electron. Agric.* **2009**, *65*, 168–175. [[CrossRef](#)]
25. Tripathi, R.; Nayak, A.K.; Shahid, M.; Lal, B.; Gautam, P.; Raja, R.; Mohanty, S.; Kumar, A.; Panda, B.B.; Sahoo, R.N. Delineation of soil management zones for a rice cultivated area in eastern India using fuzzy clustering. *Catena* **2015**, *133*, 128–136. [[CrossRef](#)]
26. Moharana, P.C.; Jena, R.K.; Pradhan, U.K.; Nogoya, M.; Tailor, B.L.; Singh, R.S.; Singh, S.K. Geostatistical and fuzzy clustering approach for delineation of site-specific management zones and yield-limiting factors in irrigated hot arid environment of India. *Precis. Agric.* **2020**, *21*, 426–448. [[CrossRef](#)]
27. Santos, R.O.D.; Franco, L.B.; Silva, S.A.; Sodré, G.A.; Menezes, A.A. Spatial variability of soil fertility and its relation with cocoa yield. *Rev. Bras. Eng. Agrícola E Ambient.* **2017**, *21*, 88–93. [[CrossRef](#)]
28. Maleki, S.; Karimi, A.R.; Zeraatpisheh, M.; Poozeshi, R.; Feizi, H. Long-term cultivation effects on soil properties variations in different landforms in an arid region of eastern Iran. *Catena* **2021**, *206*, 105465. [[CrossRef](#)]
29. Soil Survey Staff. *Keys to Soil Taxonomy*, 12th ed.; USDA-Natural Resources Conservation Service: Washington, DC, USA, 2014.
30. Ghasemzadeh Ganjehie, M.; Karimi, A.R.; Zeinadini, A.; Khorassani, R. Relationship of soil properties with yield and morphological parameters of pistachio in geomorphic surfaces of Bajestan playa, Northeastern Iran. *J. Agric. Sci. Technol.* **2018**, *20*, 417–432.
31. Page, A.L.; Miller, R.H.; Keeney, D.R. Methods of Soil Analysis. In *Chemical and Microbiological Properties, Part 2*, 2nd ed.; No. 9; ASA, SSSA, CSSA: Madison, WI, USA, 1982; pp. 595–623.
32. Nelson, D.W.; Sommers, L.E. Total carbon, organic carbon, and organic matter. Chemical and Microbiological Properties. In *Methods of Soil Analysis, Part 2*; American Society of Agronomy Inc. and Soil Science: Madison, WI, USA, 1996; pp. 961–1010.
33. Thomas, G.W. Soil pH and Soil Acidity. In *Methods of Soil Analysis, Part 3. Chemical Methods*; No. 5; American Society of Agronomy Inc. and Soil Science: Madison, WI, USA, 1996.
34. Rhoades, J. Salinity: Electrical conductivity and total dissolved solids. In *Methods of Soil Analysis, Part 3 Chemical Methods*; American Society of Agronomy Inc. and Soil Science: Madison, WI, USA, 1996; pp. 417–435.
35. Gee, G.W.; Bauder, J.W. Particle size analysis. In *Methods of Soil Analysis, Part 1*; Klute, A., Ed.; American Society of Agronomy: Madison, WI, USA, 1986; pp. 383–411.
36. Bremner, J.; Mulvaney, C. Nitrogen-total. In *Methods of Soil Analysis, Chemical and Microbiological Properties, Part 2*; American Society of Agronomy-Soil Science Society of America: Madison, WI, USA, 1982; pp. 595–624.
37. Olsen, S.R.; Sommers, L.E. Phosphorus. In *Methods of Soil Analysis, Part 2 Chemical and Microbiological Properties*; Page, A.L., Miller, H., Keeney, D.R., Eds.; American Society of Agronomy Inc. & Soil Science Society of America Inc.: Madison, WI, USA, 1982; pp. 403–429.
38. Knudsen, D.; Peterson, G.A.; Pratt, P.F. Lithium, sodium and potassium. In *Methods of Soil Analysis, Part 2 Chemical and Microbiological Properties*; Page, A.L., Miller, H., Keeney, D.R., Eds.; American Society of Agronomy Inc. & Soil Science Society of America Inc.: Madison, WI, USA, 1982; pp. 225–246.
39. Tucker, B.B.; Kurtz, L.T. Calcium and magnesium determinations by EDTA titrations. *Soil Sci. Soc. Am. J.* **1961**, *25*, 27–29. [[CrossRef](#)]
40. Vasu, D.; Kumar Singh, S.; Kumar Ray, S.; Duraisami, V.P.; Tiwary, P.; Chandran, P.; Nimkar, A.M.; Anantwar, S.G. Soil quality index (SQI) as a tool to evaluate crop productivity in semiarid Deccan plateau, India. *Geoderma* **2016**, *282*, 70–79. [[CrossRef](#)]

41. Lamichhane, S.; Kumar, L.; Wilson, B. Digital soil mapping algorithms and covariates for soil organic carbon mapping and their implications: A review. *Geoderma* **2019**, *352*, 395–413. [CrossRef]
42. Emadi, M.; Taghizadeh-Mehrjardi, R.; Cherati, A.; Danesh, M.; Mosavi, A.; Scholten, T. Predicting and Mapping of Soil Organic Carbon Using Machine Learning Algorithms in Northern Iran. *Remote Sens.* **2020**, *12*, 2234. [CrossRef]
43. Maleki, S.; Zeraatpisheh, M.; Karimi, A.; Sareban, G.; Wang, L. Assessing Variation of Soil Quality in Agroecosystem in an Arid Environment Using Digital Soil Mapping. *Agronomy* **2022**, *12*, 578. [CrossRef]
44. McBratney, A.B.; Mendonc Santos, M.L.; Minasny, B. On digital soil mapping. *Geoderma* **2003**, *117*, 3–52. [CrossRef]
45. Khaledian, Y.; Miller, B.A. Selecting appropriate machine learning methods for digital soil mapping. *Appl. Math. Model.* **2020**, *81*, 401–418. [CrossRef]
46. Taghizadeh-Mehrjardi, R.; Schmidt, K.; Toomanian, N.; Heung, B.; Behrens, T.; Mosavi, A.H.; Band, S.S.; Amirian-Chakan, A.R.; Fathabadi, A.H.; Scholten, T. Improving the spatial prediction of soil salinity in arid regions using wavelet transformation and support vector regression models. *Geoderma* **2021**, *383*, 114793. [CrossRef]
47. Zeraatpisheh, M.; Ayoubi, S.; Sulieman, M.; Rodrigo-Comino, J. Determining the spatial distribution of soil properties using the environmental covariates and multivariate statistical analysis: A case study in semi-arid regions of Iran. *J. Arid Land* **2019**, *11*, 551–566. [CrossRef]
48. Žížala, D.; Minařík, R.; Skála, J.; Bejtlerová, H.; Juřicová, A.; Reyes Rojas, J.; Penížek, V.; Zádorová, T. High-resolution agriculture soil property maps from digital soil mapping methods, Czech Republic. *Catena* **2022**, *12*, 106024. [CrossRef]
49. Kariminejad, N.; Pourghasemi, H.R.; Maleki, S.; Hosseinalizadeh, M. Digital soil mapping of exchangeable sodium percentage in loess derived-soils of Iranian Loess plateau. *Geocarto Int.* **2022**, *1*–19. [CrossRef]
50. Olaya, V.F. *A Gentle Introduction to Saga GIS*; The SAGA User Group e.V: Göttingen, Germany, 2004; p. 208.
51. Yue, J.; Tian, J.; Tian, Q.; Xu, K.; Xu, N. Development of soil moisture indices from differences in water absorption between shortwave-infrared bands. *ISPRS* **2019**, *154*, 216–230. [CrossRef]
52. APHA. *Standard Methods for the Examination of Water and Wastewater*, 9th ed.; American Public Health Association: Washington, DC, USA, 1998; p. 541.
53. Breiman, L.; Cutler, A. Random forests. *Mach. Learn.* **2001**, *45*, 5–32. [CrossRef]
54. Zhi, J.; Zhang, G.; Yang, F.; Yang, R.; Liu, F.; Song, X.; Zhao, Y.; Li, D. Predicting matic epipedons in the northeastern Qinghai-Tibetan Plateau using Random Forest. *Geoderma Reg.* **2017**, *10*, 1–10. [CrossRef]
55. R Development Core Team. *A Language and Environment for Statistical Computing*; R Foundation for Statistical Computing: Vienna, Austria, 2015. Available online: <http://www.R-project.org> (accessed on 15 December 2015).
56. Lawrence, I.; Lin, K. A concordance correlation coefficient to evaluate reproducibility. *Biometrics* **1989**, *45*, 255–268. [CrossRef] [PubMed]
57. Reddy, N.N.; Chakraborty, P.; Roy, S.; Singh, K.; Minasny, B.; McBratney, A.B.; Biswas, A.; Das, B.S. Legacy data-based national-scale digital mapping of key soil properties in India. *Geoderma* **2021**, *381*, 114684. [CrossRef]
58. Brown, D.G. Classification and boundary vagueness in mapping presettlement forest types. *Int. J. Geogr. Inf. Sci.* **1998**, *12*, 105–129. [CrossRef]
59. Minasny, B.; McBratney, A.B. *FuzMe*, Version 3.0; Australian Centre for Precision Agriculture, The University of Sydney: Sydney, Australia, 2006.
60. Jiang, H.L.; Liu, G.S.; Liu, S.D.; Li, E.H.; Wang, R.; Yang, Y.F.; Hu, H.C. Delineation of site-specific management zones based on soil properties for a hillside field in central China. *Arch. Agron. Soil Sci.* **2012**, *58*, 1075–1090. [CrossRef]
61. Behera, S.K.; Mathur, R.K.; Shukla, A.K.; Suresh, K.; Prakash, C. Spatial variability of soil properties and delineation of soil management zones of oil palm plantations grown in a hot and humid tropical region of southern India. *Catena* **2018**, *165*, 251–259. [CrossRef]
62. Barca, E.; Bruno, E.; Bruno, D.E.; Passarella, G. GTest: A software tool for graphical assessment of empirical distributions' Gaussianity. *Environ. Monit. Assess.* **2016**, *188*, 138. [CrossRef]
63. Taghizadeh-Mehrjardi, R.; Minasny, B.; Sarmadian, F.; Malone, B.P. Digital mapping of soil salinity in Ardakan region, central Iran. *Geoderma* **2014**, *213*, 15–28. [CrossRef]
64. Fathizad, H.; Ardakani, M.A.; Sodaiezadeh, H.; Kerry, R.; Taghizadeh-Mehrjardi, R. Investigation of the spatial and temporal variation of soil salinity using random forests in the central desert of Iran. *Geoderma* **2020**, *365*, 114233. [CrossRef]
65. Carter, M.R.; Gregorich, E.G. *Soil Sampling and Methods of Analysis*, 2nd ed.; CRC Press: Boca Raton, FL, USA, 2007.
66. Wilding, L.P.; Dress, L.R. Application of geostatistics to spatial studies of soil. In *Advances in Agronomy*; Trangmar, B.B., Yost, R.S., Uehara, G., Eds.; Elsevier: Amsterdam, The Netherlands, 1983; p. 38.
67. Mulder, V.L.; Lacoste, M.; Richer-de-Forges, A.C.; Martin, M.P.; Arrouays, D. National versus global modelling the 3D distribution of soil organic carbon in mainland France. *Geoderma* **2016**, *263*, 16–34. [CrossRef]
68. Gomes, L.C.; Faria, R.M.; de Souza, E.; Veloso, G.V.; Schaefer, C.E.G.R.; Filho, E.I.F. Modelling and mapping soil organic carbon stocks in Brazil. *Geoderma* **2019**, *340*, 337–350. [CrossRef]
69. Xie, X.; Wu, T.; Zhu, M.; Jiang, G.; Xu, Y.; Wang, X.; Pu, L. Comparison of random forest and multiple linear regression models for estimation of soil extracellular enzyme activities in agricultural reclaimed coastal saline land. *Ecol. Indic.* **2021**, *120*, 106925. [CrossRef]

70. Makungwe, M.; MumbiChabala, L.; Chishala, B.H.; MurrayLark, R.M. Performance of linear mixed models and random forests for spatial prediction of soil pH. *Geoderma* **2021**, *397*, 115079. [[CrossRef](#)]
71. Nabiollahi, K.; Taghizadeh-mehrjardi, R.; Shahabi, A.; Heung, B.; Amirian-Chakan, A.R.; Davari, M.; Scholten, T. Assessing agricultural salt-affected land using digital soil mapping and hybridized random forests. *Geoderma* **2021**, *85*, 114858. [[CrossRef](#)]
72. De Oliveira, J.F.; Mayi, S.; Marchão, R.L.; Corazza, E.J.; Hurtado, S.C.; Malaquias, J.V.; Tavares Filho, J.; Brossard, M.; Guimarães, M.D.F. Spatial variability of the physical quality of soil from management zones. *Precis. Agric.* **2019**, *20*, 1251–1273. [[CrossRef](#)]
73. Raiesi, F. A minimum data set and soil quality index to quantify the effect of land use conversion on soil quality and degradation in native rangelands of upland arid and semiarid regions. *Ecol. Indic.* **2017**, *75*, 307–320. [[CrossRef](#)]
74. Bhutta, M.N.; Alam, M.M. Prospectives and Limits of Groundwater Use in Pakistan. In Proceedings of the IWMI-ITP-NIH International Workshop on “Creating Synergy between Groundwater Research and Management in South and Southeast Asia”, Roorkee, India, 8–9 February 2005.
75. Oldoni, H.; Terra, V.S.S.; Timm, L.C.; Júnior, C.R.; Monteiro, A.B. Delineation of management zones in a peach orchard using multivariate and geostatistical analyses. *Soil Tillage Res.* **2019**, *191*, 1–10. [[CrossRef](#)]
76. Taghizadeh-Mehrjardi, R.; Nabiollahi, K.; Rasoli, L.; Kerry, R.; Scholten, T. Land Suitability Assessment and Agricultural Production Sustainability Using Machine Learning Models. *Agronomy* **2020**, *10*, 573. [[CrossRef](#)]
77. Gallant, J.C.; Dowling, T.I. A multi resolution index of valley bottom flatness for mapping depositional areas. *Water Resour. Res.* **2003**, *39*, 1347–1360. [[CrossRef](#)]
78. Conrad, O.; Bechtel, B.; Bock, M.; Dietrich, H.; Fischer, E.; Gerlitz, L.; Wehberg, J.; Wichmann, V.; Bohner, J. System for automated geoscientific analyses (SAGA) v. 2.1.4. *Geosci. Model Dev.* **2015**, *8*, 1991–2007. [[CrossRef](#)]
79. Moore, I.D.; Gessler, P.; Nielsen, G.; Peterson, G. Soil attribute prediction using terrain analysis. *Soil Sci. Soc. Am. J.* **1993**, *57*, 443–452. [[CrossRef](#)]
80. Bohner, J.; Selige, T. Spatial prediction of soil attributes using terrain analysis and climate regionalization. In *SAGA—Analyses and Modelling Applications*; Bohner, J., McCloy, K.R., Strobl, J., Eds.; Göttinger Geographische Abhandlungen: Göttingen, Germany, 2006; Volume 115, pp. 13–28. Available online: <https://www.semanticscholar.org/paper/Spatial-Prediction-of-Soil-Attributes-Using-Terrain-B%C3%B6hner-Selige/5c565928ba7300053348c7b95ced68c431b923b9> (accessed on 17 November 2022).
81. Allbed, A.; Kumar, L. Soil salinity mapping and monitoring in arid and semi-arid regions using remote sensing technology: A review. *Adv. Remote Sens.* **2013**, *2*, 373–385. [[CrossRef](#)]
82. Khan, N.M.; Rastoskuev, V.V.; Sato, Y.; Shiozawa, S. Assessment of hydrosaline land degradation by using a simple approach of remote sensing indicators. *Agricult. Water Manag.* **2005**, *77*, 96–109. [[CrossRef](#)]
83. Douaoui, A.E.K.; Nicolas, H.; Walter, C. Detecting salinity hazards within a semiarid context by means of combining soil and remote-sensing data. *Geoderma* **2006**, *134*, 217–230. [[CrossRef](#)]
84. Ray, S.S.; Singh, J.P.; Das, G.; Panigrahy, S. Use of high resolution remote sensing data for generating site-specific soil management plan. *Int. Arch. Photogramm. Remote Sens. Spatial Inf. Syst. B* **2004**, *35*, 127–131.
85. Arzani, H.; King, G.W. Application of Remote Sensing (Landsat TM Data) for Vegetation Parameters Measurement in Western Division of NSW; International Grassland Congress: Hohhot, China, 2008; ID NO. 1083.
86. Chen, Y.; Qiu, Y.; Zhang, Z.; Zhang, J.; Chen, C.; Han, J.; Liu, D. Estimating salt content of vegetated soil at different depths with Sentinel-2 data. *Peer J.* **2020**, *8*, e10585. [[CrossRef](#)]
87. Huete, A.R.; Didan, K.; Miura, T.; Rodriguez, E.P.; Gao, X.; Ferreira, L.G. Overview of the radiometric and biophysical performance of the MODIS vegetation indices. *Remote Sens. Environ.* **2002**, *83*, 195–213. [[CrossRef](#)]
88. Rondeaux, G.; Steven, M.; Baret, F. Optimization of soil adjusted vegetation indices. *Remote Sens. Environ.* **1996**, *50*, 95–107. [[CrossRef](#)]
89. Rouse, J.W.; Haas, J.R.H.; Schell, J.A.; Deering, D.W. Monitoring vegetation systems in the Great Plains withers. In Proceedings of the 3rd ERTS Symposium, Washington, DC, USA, 10–14 December 1974.
90. Jordan, C.F. Derivation of leaf area index from quality of light on the forest floor. *Ecology* **1969**, *50*, 663–666. [[CrossRef](#)]
91. Zinck, J.A. Physiography and Soils. Lecture Notes for Soil Students, Soil Science Division, Soil Survey Courses Subject Matter, K6 ITC, Enschede, The Netherlands, 1989. Available online: [https://webapps.itc.utwente.nl/librarywww/papers\\_1989/tech\\_zinck\\_phys.pdf](https://webapps.itc.utwente.nl/librarywww/papers_1989/tech_zinck_phys.pdf) (accessed on 17 November 2022).
92. Toomanian, N.; Jalalian, A.; Khademi, H.; Karimian Eghbal, M.; Papritz, A. Pedodiversity and pedogenesis in Zayandeh-rud Valley, central Iran. *Geomorphology* **2006**, *81*, 376–393. [[CrossRef](#)]

**Disclaimer/Publisher’s Note:** The statements, opinions and data contained in all publications are solely those of the individual author(s) and contributor(s) and not of MDPI and/or the editor(s). MDPI and/or the editor(s) disclaim responsibility for any injury to people or property resulting from any ideas, methods, instructions or products referred to in the content.